SOFT ROBOTICS
Volume 00, Number 00, 2020

DOI: 10.1089/soro.2019.0082

SoRo
Soft Robotics

Octopus Arm-Inspired Tapered Soft Actuators with Suckers for Improved Grasping

Zhexin Xie,[1,2,*] August G. Domel,[3,*] Ning An,[3] Connor Green,[3] Zheyuan Gong,[1] Tianmiao Wang,[1] Elias M. Knubben,[4] James C. Weaver,[5] Katia Bertoldi,[3] and Li Wen[1]

Abstract

Octopuses can employ their tapered arms to catch prey of all shapes and sizes due to their dexterity, flexibility, and gripping power. Intrigued by variability in arm taper angle between different octopus species, we explored the utility of designing soft actuators exhibiting a distinctive conical geometry, compared with more traditional cylindrical forms. We find that these octopus-inspired conical-shaped actuators exhibit a wide range of bending curvatures that can be tuned by simply altering their taper angle and they also demonstrate greater flexibility compared with their cylindrical counterparts. The taper angle and bending curvature are inversely related, whereas taper angle and applied bending force are directly related. To further expand the functionality of our soft actuators, we incorporated vacuum-actuated suckers into the actuators for the production of a fully integrated octopus arm-inspired gripper. Notably, our results reveal that because of their enhanced flexibility, these tapered actuators with suckers have better gripping power than their cylindrical-shaped counterparts and require significantly larger forces to be detached from both flat and curved surfaces. Finally, we show that by choosing appropriate taper angles, our tapered actuators with suckers can grip, move, and place a remarkably wide range of objects with flat, nonplanar, smooth, or rough surfaces, as well as retrieve objects through narrow openings. The results from this study not only provide new design insights into the creation of next-generation soft actuators for gripping a wide range of morphologically diverse objects but also contribute to our understanding of the functional significance of arm taper angle variability across octopus species.

Keywords: octopus arm, tapered soft actuator, bending and suction

Objective

Biological systems have inspired the design of a wide range of materials and devices capable of addressing modern engineering challenges.[1–8] Octopuses represent one such example. They can effectively catch prey of different shapes and sizes, perform remarkably complex tasks, and retrieve objects from constrained environments by combining two important capabilities: (1) the ability to control many degrees of freedom and (2) the integration of linear arrays of suckers (Fig. 1A–C).[9–14] Because of their flexibility, agility, and adaptability for efficiently grasping a wide range of structurally diverse objects, octopus arms have served as model systems for the development of robust soft robotic prototypes. These range from single powerful actuators[15–19] to more complex multi-actuator systems.[20–24] These soft robots offer many advantages over their more traditional rigid counterparts in that they are significantly easier and cheaper to manufacture, are safer to operate around human subjects, and can achieve complex outputs with simple inputs.[25–35] Despite the fact that octopus arms exhibit a characteristic conical geometry and that the taper angle is highly variable between different species, many soft actuators (including octopus-inspired forms) exhibit a constant cross-

[1]School of Mechanical Engineering and Automation, Beihang University, Beijing, China.
[2]Shenyuan Honors College, Beihang University, Beijing, China.
[3]John A. Paulson School of Engineering and Applied Sciences, Harvard University, Cambridge, Massachusetts.
[4]Leitung Corporate Bionic Department, Festo SE & Co. KG, Germany.
[5]Wyss Institute of Biologically Inspired Engineering, Harvard University, Cambridge, Massachusetts.
*These authors contributed equally to this work.

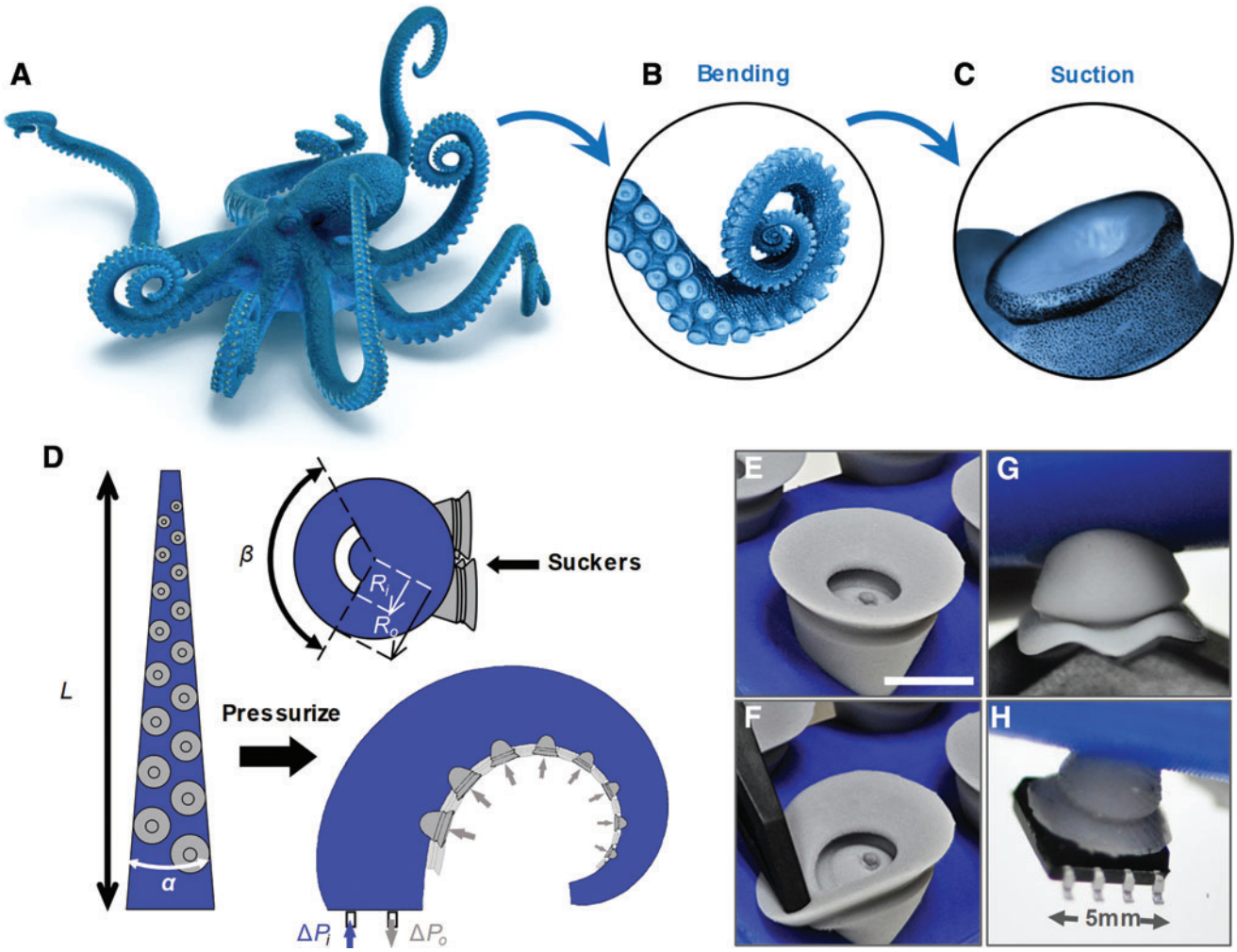

FIG. 1. Octopus arm-inspired tapered soft actuators with suckers for improved grasping. **(A–C)** Octopus arms are tapered and incorporate both bending and suction functionalities. Here, we use them as inspiration for the design of soft robotic actuators with improved grasping. **(D)** Schematics of our tapered soft actuators with suckers. **(E–H)** Our suckers are flexible, conformable, and can attach to small objects. Scale bar in panel **(E)**, 1 cm. Color images are available online.

sectional diameter along their length.[24,27–31] Little is known regarding the functional significance of this diversity, however, as previous studies on octopus-inspired tapered soft actuators have focused on the control of the arm motion.[15–22] While the subject of modeling passive bending of tapered cantilever beams has received some attention,[36] little research has been done on soft robotics which can grasp or manipulate objects.

Inspired by investigations into the morphological diversity of octopus arms, we explore the potential trade-offs between dexterity and gripping power in tapered soft actuators. In contrast to previous studies on octopus-inspired robots, which focused primarily on either arm motion[15–22] or sucker action alone,[37–40] in this study we focus on the (1) tapered arm and (2) the synergistic function of bending and suction. We first numerically study the bending kinematics and applied forces of tapered soft actuators, and then use these findings to guide the design and fabrication of an octopus arm-inspired soft robot with integrated suckers for improved gripping (Fig. 1D–H).

Materials and Methods

Details on the measurements performed to estimate the taper angle of living specimens can be found in Section S1 of the Supplementary Data. The design geometry of the tapered actuator and its suckers investigated in this study is detailed in Section S2 of the Supplementary Data. The fabrication details of the tapered soft actuators used in the validation of the finite element (FE) simulations and the characterization of the material mechanical response can be found in Section S3 of the Supplementary Data. The bending curvature and bending force experiments on tapered soft actuators without suckers can be found in Section S4 of the Supplementary Data. The FE simulations for bending curvature and applied bending force were conducted with Abaqus (SIMULIA, Providence, RI), and details can be found in Section S5 of the Supplementary Data. Using the insights from the results of the FE simulations, the tapered actuators with suckers were ultimately fabricated with a multistep molding and casting process. The tapered soft actuators were made of Mold Star

30 (Smooth-On, Inc., PA), and the suckers were made of Dragon Skin FX-Pro (Smooth-On, Inc.). Details for this fabrication can be found in Section S6 of the Supplementary Data. The experiments of sucker attachment forces are detailed in Section S7 of the Supplementary Data. And finally, demonstrations of the complete tapered actuators with suckers can be found in Section S8 of the Supplementary Data.

Results

Octopus arms

In this study, we focus on two important features of octopus arms: the taper angle and the combination of arm bending and suction. Since a systematic investigation on the taper angle range of octopus arms was not available to guide our study, we performed detailed measurements from online photographs of living specimens[41] acquired from 10 different octopus species (Section S1 of the Supplementary Data and Supplementary Fig. S1). While there are extremes in arm taper angle, such as the exceptionally broad arms found in *Abdopus gorgonos*, we found that for most species, arm taper angles ranged from a minimum of ca. 3° for the very slender arms of *Octopus macropus* to a maximum of ca. 13.5° for the comparatively broader arms found in *Eledone cirrhosa* (Fig. 2, see Supplementary Table S1 for detailed data). Guided by these measurements, we considered taper angles ranging from $\alpha = 3°$ to $\alpha = 13.5°$ and investigated their effects on both actuator bending curvature and applied bending force in the present study.

In most octopus species, two rows of suckers are distributed in a staggered arrangement along the ventral surface of each arm, with diameters ranging from a few millimeters to a few centimeters.[11,42] They comprise an exposed disk-like *infundibulum* and a central cavity *acetabulum* and allow for strong attachment not only to large flat surfaces but also to irregular surfaces, and even objects smaller than a single sucker.[43,44] In this study, we mimicked this general structure and distribution when designing our soft robotic suckers for integration into our tapered soft actuators. Although much simpler than their natural counterpart, these biomimetic suckers provide a similar function. Upon application of vacuum, they enable the actuator to attach to arbitrary objects.

Effect of taper angle on bending curvature and applied bending force

We first investigated, numerically, via FE simulations, the properties of tapered pneumatic soft actuators (without suckers), focusing on the effect of the taper angle on both bending curvature and applied bending force. Specifically, we considered tapered soft actuators, each of the same length ($L = 200$ mm) and tip diameter ($D_{tip} = 8.4$ mm), but with taper angles ranging from $\alpha = 3°$ to $\alpha = 13.5°$ (see Section S2 of the Supplementary Data for more design details). To induce bending via inflation, a single hollow internal chamber was placed along the length of the actuator at a fixed normalized distance from the outer radius of the actuator. The internal chamber was tapered in the same manner as that of the actuator, and the cross-sectional shape of the chamber was annular, swept 120° (see Section S2 of the Supplementary

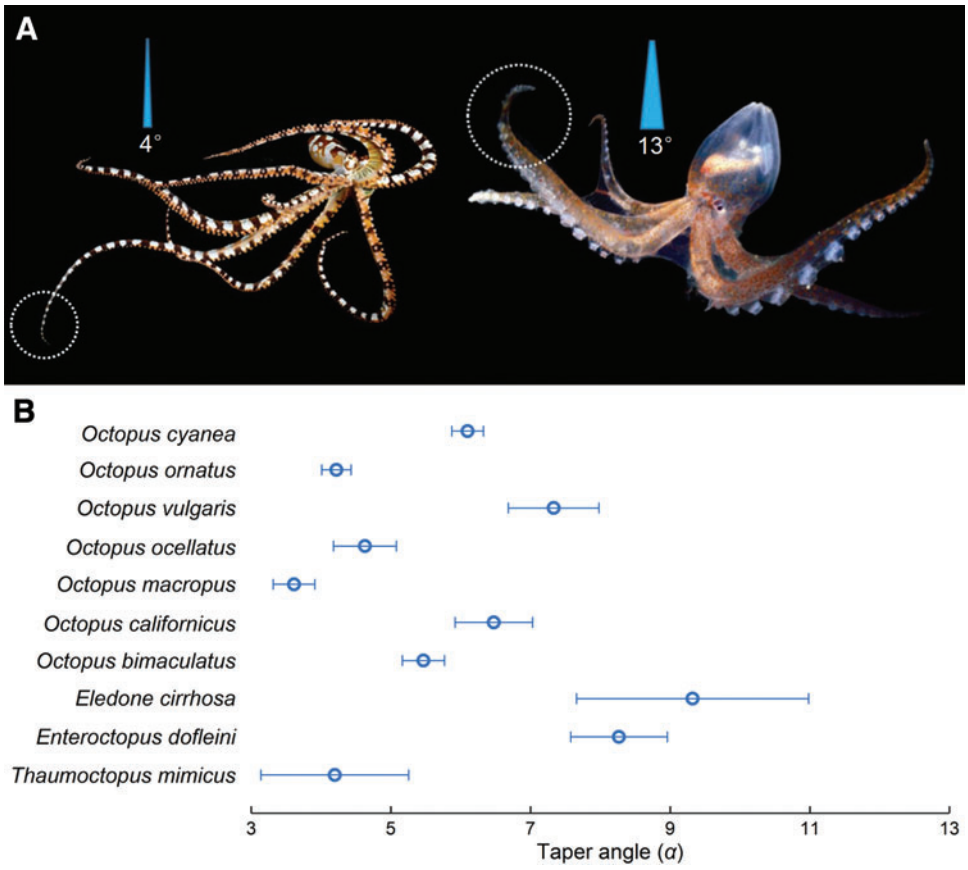

FIG. 2. Arm taper angle diversity among various octopus species. **(A)** Photographs of two representative octopus species that exhibit low (*left*, *Wunderpus photogenicus*) and high (*right*, *Vitrelladonella richardi*) arm taper angles. **(B)** Taper angle measurements (all data are provided in Supplementary Table S1) from 10 different octopus species (multiple individuals of each species were considered). Octopus photos courtesy of Roy Caldwell and Solvin Zankl. Color images are available online.

Data and Supplementary Fig. S3 for more details and schematics on the internal chamber).

For FE studies, all models were constructed using 8-node linear brick elements (Abaqus element type C3D8H), and the material behavior was captured using an incompressible Gent model,[45] with initial shear modulus $\mu = 195$ kPa and stiffening parameter $J_m = 12$ (see Section S3 of the Supplementary Data for more details). Static nonlinear simulations were performed using Abaqus/Standard and, to induce bending, each actuator's inner chamber was pressurized from $P = 0$ kPa to $P = 200$ kPa with the bottom end of the actuator being held in a fixed position. To evaluate the effect of the taper angle on the bending curvature, no additional constraint was added, and at each incremental 2 kPa increase in pressure, the maximum, minimum, and average curvature along the bending profile of the actuator was measured (see Section S4 of the Supplementary Data for more details). To study the effect of taper angle on applied bending force, the actuators were placed at a horizontal distance $d = 30$ mm away from a rigid body surface (representing a hypothetical load cell) and frictional surface to surface contact (with a coefficient of friction of 0.5) was employed between the actuator and the hypothetical load cell. When an input pressure was applied to each of these actuators (with the actuator base fixed), they would bend toward this rigid surface and the applied force was monitored.

We first validated our numerical simulations by comparing the numerical results with those obtained experimentally for actuators fabricated from Mold Star 30 (Smooth-On, Inc.) silicone rubber (Sections S4 of the Supplementary Data and Supplementary Figs. S12 and S14). Since we found an excellent agreement between the two data sets in terms of both bending curvature and bending force over a wide range of pressures, we then proceeded to use FE simulations for a much more extensive exploration of the actuator design space. We started by numerically investigating the effect of the taper angle on the bending curvature. The results shown in Figure 3A demonstrate that the bending curvature of the tapered actuators depend highly on both the taper angle α and the pneumatic pressure P. Specifically, the bending curvature increases as pressure P increases, but decreases as the taper angle α increases. For example, the average bending curvature (κ) decreased by over twofold (from $\kappa = 0.0282\ \text{mm}^{-1}$ to $\kappa = 0.0134\ \text{mm}^{-1}$) by increasing the taper angle from $\alpha = 3°$ to $\alpha = 13.5°$ at $P = 200$ kPa, and changed from $\kappa = 0.0009\ \text{mm}^{-1}$ to $\kappa = 0.0134\ \text{mm}^{-1}$ by increasing the pneumatic pressure from $P = 100$ kPa to $P = 200$ kPa for $\alpha = 13.5°$ (see Section S5 of the Supplementary Data and Supplementary Fig. S13 for more detailed simulation results of bending curvature). It should also be noted that for a given pressure and taper angle, the maximum, minimum, and average curvatures varied along the length of the actuator, thus permitting the grasping of different sized objects at a single actuating pressure.

After characterizing bending curvature as a function of taper angle, we next investigated the exerted bending force as a function of pressure. Interestingly, the numerical results reported in Figure 3B show that the taper angle produced opposite responses in terms of bending force and bending curvature (Fig. 3B and see Section S4 of the Supplementary Data and Supplementary Fig. S11 for results of other measured distances other than $d = 30$ mm). For example, the bending force increased from 0.33 to 5.35 N when the taper angle was increased from $\alpha = 3°$ to $\alpha = 13.5°$ at $P = 200$ kPa (Fig. 3B), whereas the bending curvature decreased from $\kappa = 0.0282\ \text{mm}^{-1}$ to $\kappa = 0.0134\ \text{mm}^{-1}$ when the taper angle was increased from $\alpha = 3°$ to $\alpha = 13.5°$ at $P = 200$ kPa (Fig. 3A). Therefore, when taking both the bending force and bending curvature results into account, we discovered an inherent trade-off between the two. Overall, models with lower taper angles output a lower force but could bend with much larger curvature (with the opposite being true for larger taper angles).

The complete octopus arm-inspired prototype

Guided by these numerical results, we then investigated how the taper angle affected the gripping power of a soft actuator with integrated suckers. To this end, 17 silicone rubber suction cups (made from Dragon Skin FX-Pro; Smooth-On, Inc.) were integrated into the design using a multistep molding process and arranged in a staggered

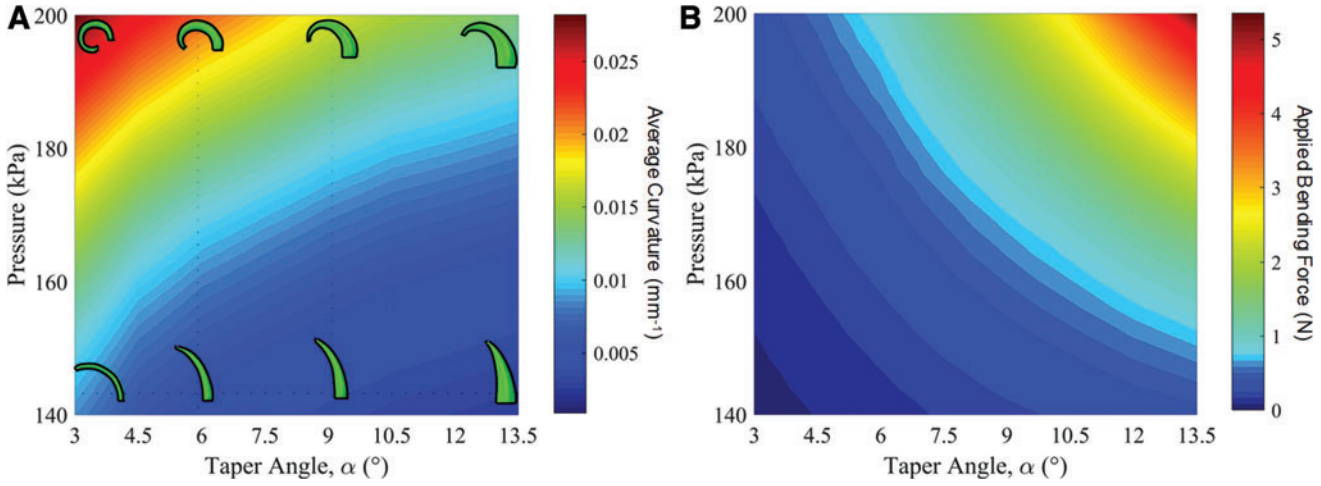

FIG. 3. Modeling the effects of arm taper angle on bending curvature and applied bending force. **(A)** Numerical results illustrating the average bending curvature (κ) as a function of taper angle (α) and input pressure (P). Bending profile snapshots obtained from the simulations at $P = 150$ kPa and $P = 200$ kPa are overlaid on the heat map. **(B)** Numerical results illustrating the applied bending force (FN) as a function of taper angle (α) and input pressure (P). Color images are available online.

pattern along the length of the actuator (Fig. 1 and Section S6 of the Supplementary Data and Supplementary Fig. S15). The flexible suckers were designed and fabricated by mimicking the geometries of the *infundibulum* and *acetabulum* of *Octopus vulgaris* (Fig. 1C).[46] Moreover, for the sake of simplicity, they were all connected to a single-channel vacuum generator which was used to lower the pressure inside each of the suckers. Upon evacuation, the suckers could conform and attach to a wide range of different-sized objects (Fig. 1H), and even those with irregular surfaces (Fig. 1G). We constructed both a cylindrical and an $\alpha = 9°$ tapered actuator with suckers and characterized the attachment behavior of their suckers to substrates exhibiting a variety of different geometries and surface roughnesses (see Section S7 of the Supplementary Data for details). Note that in the tapered gripper, the size of the suction cups decreased from the base of the actuator to the tip, as is seen in its biological counterpart (Supplementary Fig. S4). In contrast, the cylindrical gripper used suction cups which were all identical and dimensionalized to provide the same total suction area as in the tapered gripper (Supplementary Fig. S5).

Attachment abilities characterization

We began by characterizing the attachment of the cylindrical and tapered grippers to planar substrates (Fig. 4A) since planar objects are often difficult to grasp using bending actuators alone. In these tests, we first lowered the pressure inside the suckers from 0 to −80 kPa to fully attach the suction cups to the surface and then pulled the grippers in the direction perpendicular to the surface while recording the force via a substrate-integrated load cell. Remarkably, we found that the enhanced flexibility of the tapered gripper results in significantly higher gripping power. Specifically, the results shown in Figure 4A–C show two key features. First, the pull-off force (i.e., the maximum force recorded during the test) recorded for a tapered gripper (6.59 ± 0.32 N) is significantly higher than that measured for the cylindrical one (5.61 ± 0.24 N) (Fig. 4C). Second, the mechanism by which the two grippers eventually detach from the surface is qualitatively different. While suckers of the tapered gripper detached from the surface in a sequential manner (Fig. 4A, B, Supplementary Movies S1 and S2), resulting in a post-yield stairstep-like

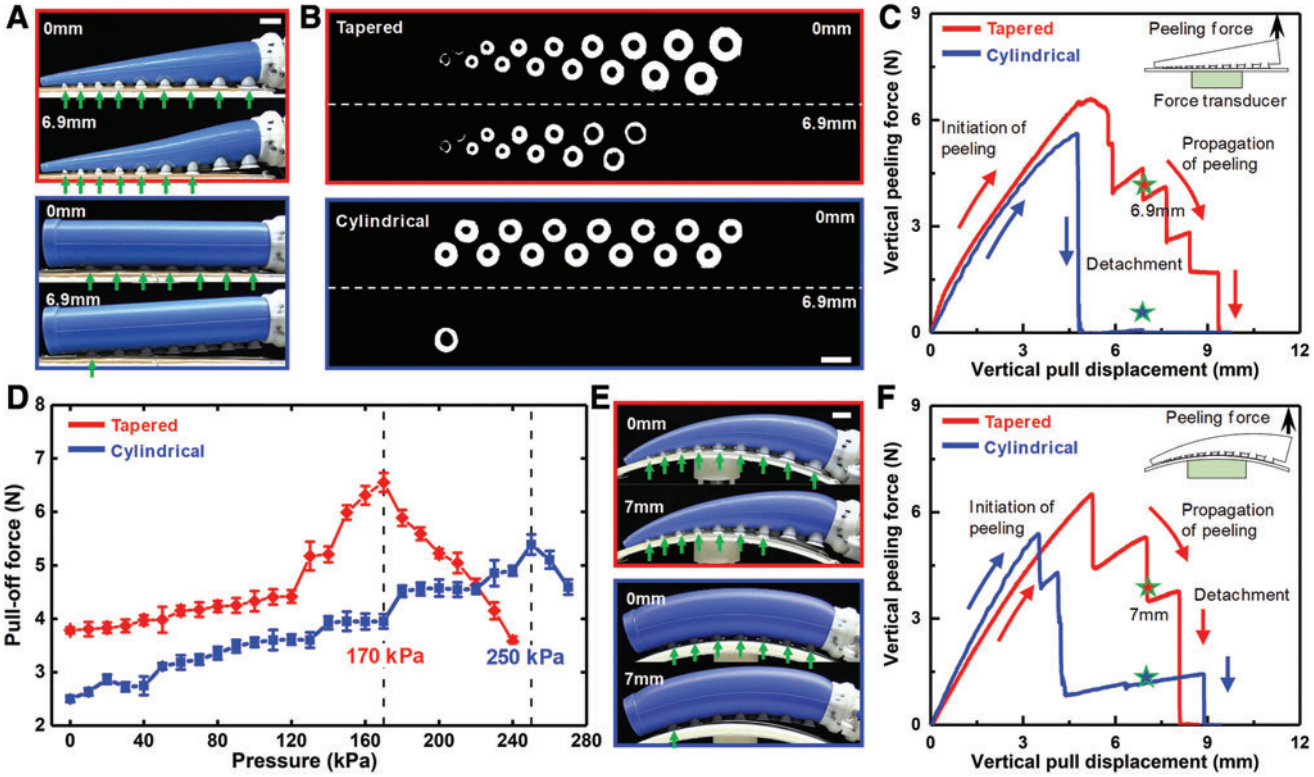

FIG. 4. Sucker attachment force and contact measurements. **(A)** Side view photographs showing the sequential peeling of the tapered ($\alpha = 9°$) actuator with suckers, and the simultaneous peeling of the cylindrical actuator with suckers from a smooth planar surface (scale bar, 20 mm). The *blue arrows* indicate the suckers that are attached to the surface during peeling. **(B)** Frustrated total internal reflection[47] images highlighting the attachment of the suckers (see also Supplementary Movie S2) (scale bar, 20 mm). **(C)** Load–displacement curves recorded during the peeling test for both the tapered and cylindrical actuators with suckers. The peeling force is measured along the vertical direction. **(D)** Scanning a wide range of input pressures permits the identification of the optimal input pressures for maximizing pull-off forces of both actuators with suckers from nonplanar substrates. The *vertical dashed line* indicates the ''optimal'' pneumatic pressure values for maximizing the pull-off forces for the curvature of this specific surface ($260\ \text{mm}^{-1}$). **(E)** Side view photographs showing the sequential peeling of an $\alpha = 9°$ actuator with suckers, and the almost simultaneous peeling of the cylindrical actuator with sucker from a smooth curved surface (scale bar, 20 mm). **(F)** Load–displacement curves recorded during the peeling test for both the tapered and cylindrical actuators with suckers. The peeling force is measured along the vertical direction. Color images are available online.

failure mode (Fig. 4C), the reduced flexibility of the cylindrical one prevented such behavior and led to simultaneous detachment of all suckers (Fig. 4A, B, Supplementary Movies S1 and S2), inducing a sharp drop in force (Fig. 4C).

We next characterized the attachment abilities of the actuators with suckers to curved surfaces and focused on a surface with curvature 1/260 mm^{-1}. The results shown in Figure 4D demonstrate that the attachment to the surface for both the tapered and cylindrical grippers was highly dependent on the pressure, with the maximum pull-off forces recorded at $P = 170$ and 250 kPa, respectively. When such pressure is applied, the actuators best approximated the curved surface, and the suckers were fully engaged and provided maximum gripping power. Notably, in this case we found that the enhanced flexibility of the tapered actuator resulted in a larger maximum pulling force (6.55 ± 0.18 N). It is also important to note that both soft grippers could achieve almost identical pull-off force on the flat and curved surfaces (Fig. 4C, F). This behavior was enabled by the intrinsic compliance of the actuators that allowed them to conform to arbitrarily shaped objects so that all suckers could engage with the surface. To completely eliminate the impact of the sucker size and distribution on the attachment performance, we also tested a cylindrical gripper with suckers of identical size and distribution to those of our tapered design. As shown in Supplementary Figure S19, we found that in this case also, all the cylindrical gripper suckers peeled off nearly simultaneously, resulting in a sharper and more sudden failure compared with the tapered design. These results further support our conclusion that the tapered actuator with suckers has better gripping power than its cylindrical counterpart.

Due to their compliant nature, the suckers were also able to successfully attach to surfaces exhibiting a wide range of surface roughnesses (Fig. 5A–C), but exhibited pronounced performance trade-offs which varied as a function of sucker modulus. For example, the $\alpha = 9°$ gripper with stiff suckers (Young's modulus 660 kPa) generated a considerable pull-off force of up to 26.14 ± 0.54 N (error values ± standard error of the mean) on relatively smooth surfaces (R_a <20 μm), which represented a nearly fourfold increase over that of the $\alpha = 9°$ gripper with flexible suckers (Young's modulus 250 kPa) (Fig. 5D). Despite this performance advantage on smooth surfaces, and due to their reduced flexibility, the stiffer suckers exhibited a reduced ability to conform to more topographically complex surfaces (e.g., $R_a = 200$ μm in Fig. 5), highlighting the need to consider sucker modulus when exploring the suitable application space of the gripper.

Grasping applications

After characterizing the sucker's capabilities and required peeling forces, we explored the real-world applications of our tapered grippers. Given the observed trade-off between bending curvature and bending force, one could select either a taper angle that places a premium on bending curvature or bending force or a taper angle that balances both at moderate levels. In this study, we chose: (1) an intermediate taper angle ($\alpha = 9°$) that leads to a good balance between high force application and moderate bending curvature and (2) a relatively small taper angle ($\alpha = 4.5°$) that places a premium on bending curvature over applied bending force (attachment force of the $\alpha = 4.5°$ gripper against different surfaces is provided in Supplementary Fig. S18).

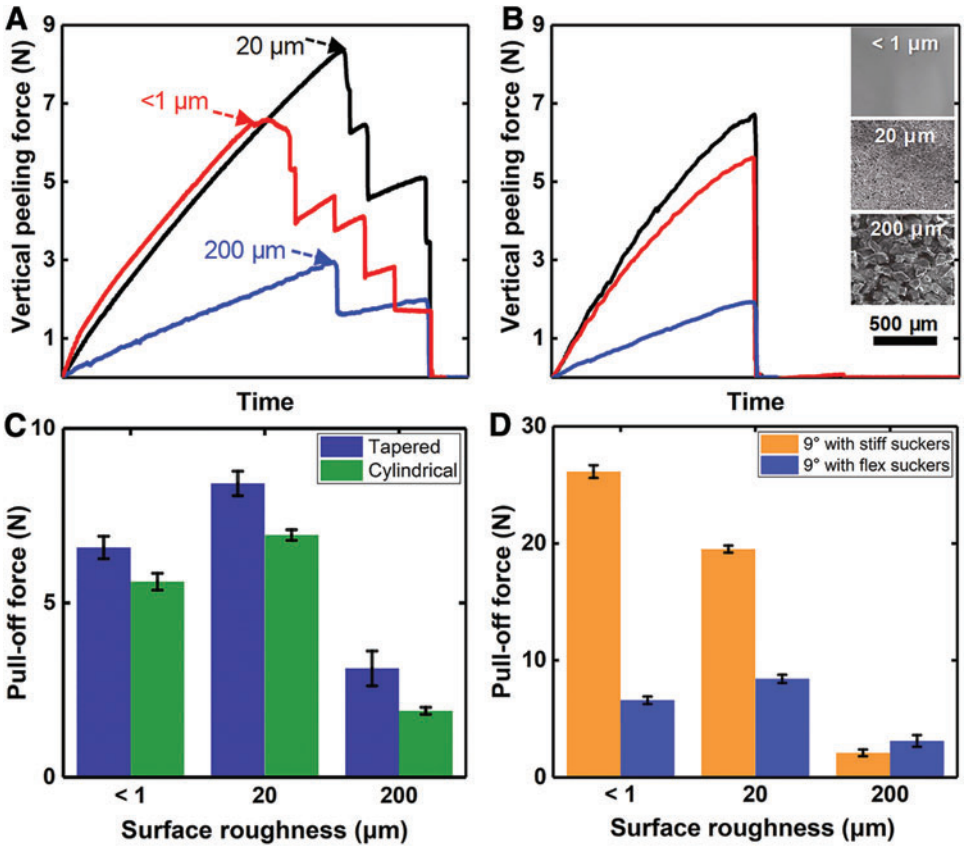

FIG. 5. Attachment force of the $\alpha = 9°$ tapered gripper and its corresponding cylindrical gripper against different surfaces. Soft sucker (Young's modulus: 260 kPa) vertical peeling forces plotted against time for surfaces of various roughnesses (R_a: <1, 20, 200 μm) for **(A)** the $\alpha = 9°$ tapered gripper and **(B)** its corresponding cylindrical gripper, demonstrating the stair step-like failure mode of the tapered actuator **(A)**. The corresponding scanning electron microscopic images for the different surfaces are shown in **(B**, *inset*). **(C)** The attachment forces of the $\alpha = 9°$ gripper and its corresponding cylindrical gripper on planar surfaces of various roughnesses (R_a: <1, 20, 200 μm). **(D)** The attachment forces of the $\alpha = 9°$ gripper with stiff (Young's modulus: 660 kPa) and flexible suckers (Young's modulus: 260 kPa) on planar surfaces of various roughnesses (R_a: <1, 20, 200 μm). Color images are available online.

We first demonstrated the abilities of our tapered grippers to attach, wrap, transport, and deliver an object of interest, which necessitated the use of both bending and suction functionalities (Fig. 6A). Specifically, a thin plastic sheet was grasped from an initially planar geometry and then transported and delivered in a rolled-up orientation—an operation that could be useful in assembly line applications involving thin membranes. In this example, the gripper characterized by $\alpha = 4.5°$ was able to move the thin sheet in three steps (Fig. 6A and Supplementary Movie S3): (1) starting with the nonpressurized gripper (0 s), the suction cups made contact with the planar surface and a vacuum was applied. (2) Once the system detected the pressure change from the suckers, the robotic arm lifted the sheet to a predefined height above the workspace (4 s). At $\sim$6 s (a preset time delay), the gripper was then pressurized ($P = 250$ kPa) to ''wrap'' the sheet into a roll (6.5 s). (3) The robotic arm transported the sheet quickly (8 s) and at a constant speed and then delivered it to a human hand at 12 s (by releasing the vacuum and inflation pressure). Supplementary Figure S20 shows the inflation and vacuum pressures as a function of time during this process. Based on the pressure sensory feedback, the ''attach, wrap, transport, and deliver'' motion could be utilized in a semiautonomous way and could achieve safe and efficient assistance when interacting with a human subject. We also want to point out that we repeated the ''attach, wrap, transport, and deliver'' experiment 20 times and observed a 100% success rate, demonstrating the robustness of our system. Similar results were also observed with the $\alpha = 9°$ gripper, but the wrapping abilities were reduced based on the actuator's larger taper angle leading to smaller curvatures (Supplementary Movie S5).

To further expand on the practical applications of our design, we sought to create a seamless human–machine interface to control pressurization and depressurization. As an initial proof of concept, we constructed a device that integrated a pressurization valve and vacuum generator into a bulb-shaped handle (60 mm in diameter), with two buttons operable by a single human hand (Fig. 6B). Using this bulb-shaped handle, we then examined the prototype's ability to grasp common objects (Fig. 6C). Both the $\alpha = 4.5°$ and the $\alpha = 9°$ handheld prototypes

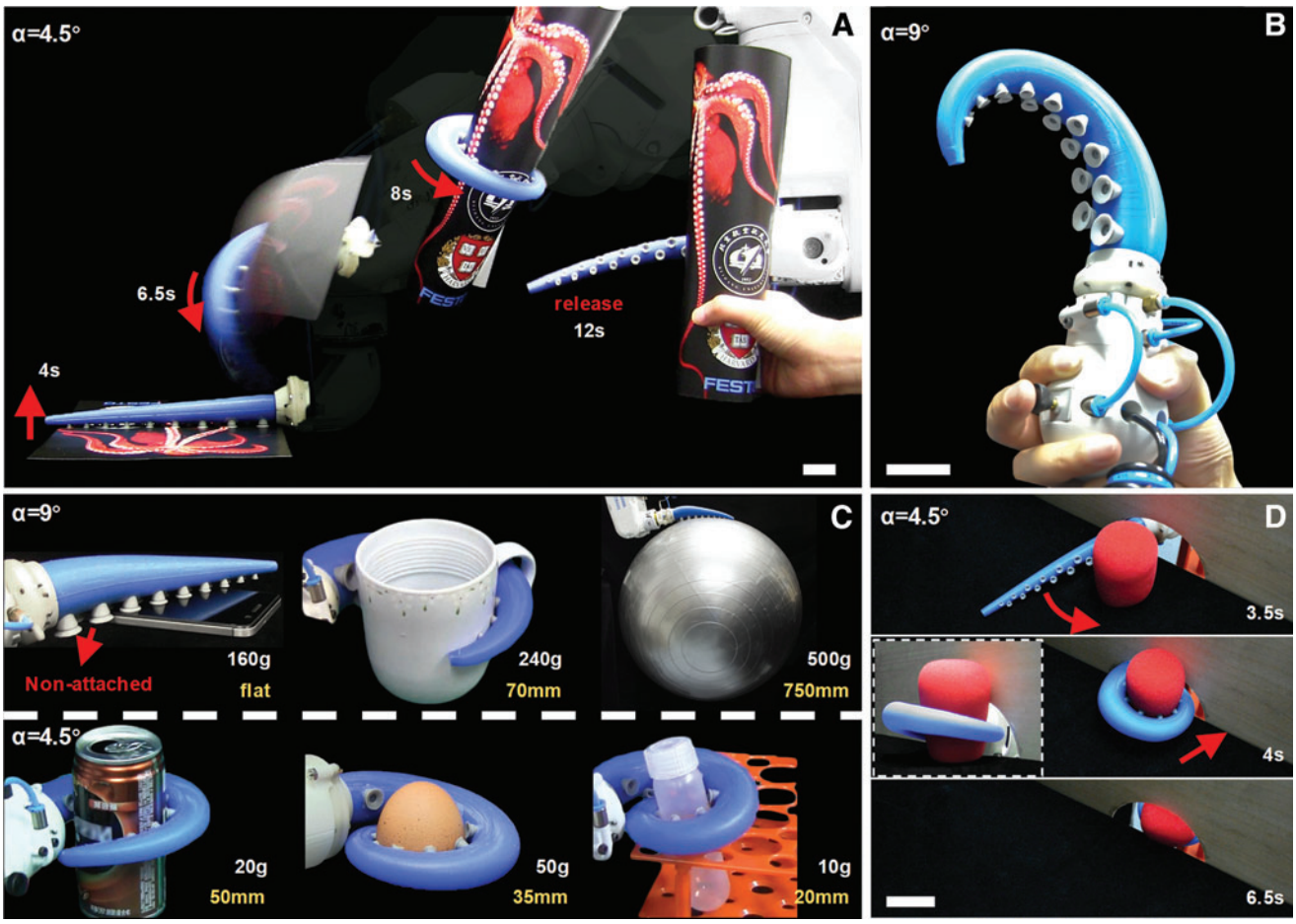

FIG. 6. Exploring the application space for the tapered grippers. **(A)** Suction and bending for picking up, rolling, and placing a printed plastic sheet (see Supplementary Fig. S20 for details of its pressure control). This specific task is termed ''attach, wrap, transport, and deliver''—a video of which is available in Supplementary Movie S3 (scale bar, 30 mm). **(B)** In a modified configuration, a two-button bulb-like controller that integrates a pressure valve and vacuum regulator is used, allowing for simple, one-hand operability (scale bar, 30 mm). **(C)** The tapered grippers can grip a wide range of objects via this handheld controller. *Upper row*: $\alpha = 9°$ gripper; *lower row*: $\alpha = 4.5°$ gripper. Video documentation of these actions are provided in Supplementary Movies S4 and S5. The weights and sizes of the objects are indicated for each grasped object. **(D)** The tapered gripper retrieving objects from confined spaces—a video of which is available in Supplementary Movie S8 (scale bar, 30 mm). Color images are available online.

were able to adequately grasp objects, such as a test tube (with a diameter of 20 mm), a mug (with a diameter of 70 mm), or a yoga ball (with a diameter of 750 mm); however, each actuator clearly has its strengths and weaknesses based on the previously observed trade-offs between curvature and applied bending force. The tapered gripper with $\alpha = 4.5°$, for example, was able to more easily grasp the light weight items with higher curvatures, such as the can, egg, and test tube, whereas the $\alpha = 9°$ gripper struggled to do so (Fig. 6C and Supplementary Movies S4 and S5). This observation is due to the fact that the actuator with $\alpha = 4.5°$ can bend into a larger curved state (a spiral shape with the tip of the actuator curling past its base) than the actuator with $\alpha = 9°$ (Supplementary Fig. S21A and Supplementary Movies S6 and S7). However, the $\alpha = 9°$ gripper was able to more easily grasp the heavier and bulkier objects with lower curvatures, such as the mug and yoga ball (Fig. 6C), and a bucket of water weighing up to 27 N, which is over 24 times the weight of the gripper (Supplementary Fig. S21B). Moreover, the $\alpha = 9°$ gripper was capable of gripping a cell phone even when some of the suction cups are nonattached to the surface (Fig. 6C). These results confirm that the combination of bending (with choosing the appropriate taper angle) and suction can allow for the grasping of an extremely wide range of objects, including planar and nonplanar geometries, rigid and soft, and rough and smooth objects.

Since octopuses are well known for the ability to retrieve objects from confined spaces by adaptively deforming the arm when going through/out a small opening,[48] we also investigated whether our octopus-inspired actuator with suckers could perform similar functions. To carry out these studies, we considered a wall with a 4 cm diameter hole and then placed a deformable object measuring 8 cm in height on one side (Fig. 6D) and the $\alpha = 4.5°$ gripper (which was barely small enough to fit through the opening) connected to a robotic arm (MOTOMAN MH3F; YASKAWA, Inc., Japan) on the other side (Supplementary Movie S8). The enhanced flexibility provided by the tapered design enabled the gripper to extend almost its entire length through the opening (3.5 s), to fetch a squishy object (4 s), and to return through the small opening with the object (6.5 s). The successful demonstration of this retrieving behavior was only possible with our streamlined tapered design and thus highlights the further usefulness of this conical geometry for object manipulation in constrained environments. We also mounted the gripper on an elephant trunk-like (or octopus arm-like) appendage (Supplementary Movie S9) to demonstrate a large-scale continuum of motion in three-dimensional space that could be safely operated in the company of human bystanders.

Conclusions

In the present report, we used a combination of numerical analyses and experiments to investigate the response of tapered octopus-inspired soft actuators. We found that, in contrast to typical soft actuators with a cylindrical shape that bend with a constant curvature,[24,27–31] the tapered actuators considered in this study could achieve nonconstant bending curvature along their lengths and a more spiral-like shape (Supplementary Fig. S22). Guided by the numerical analyses, we then designed and fabricated a multifunctional tapered gripper and evaluated its gripping ability over a wide range of structurally diverse objects. Importantly, we found that the enhanced flexibility of the tapered design translated into higher gripping power. Surprisingly, through the combined action of bending and suction, our tapered gripper could easily grip a variety of flat, curved, smooth, and rough items, ranging in diameter from 5 mm (Fig. 1H) to 750 mm (Fig. 6C) and weights up to 27 N (Supplementary Fig. S21B). The varying bending curvature along the length is an intriguing and potentially useful phenomenon in that it enables gripping of objects of significantly smaller sizes than those typically manipulated employing a nontapered geometry.

The pneumatic pressure input (and the resulting bending curvature) was also seen to play an important role in the interfacial attachment of the suckers to nonplanar surfaces and could thus be employed to maximize the attachment performance of the suckers to such surfaces. As a result, and in contrast to previously documented soft actuators employing other mechanisms of biologically inspired adhesion,[49–52] our tapered actuators with suckers can easily grip a variety of flat, curved, smooth, and rough items through the combined action of bending and suction. Compared with grippers that require several actuators organized into a hand-like geometry,[27,33,34,37,53] our system requires only a single actuator to complete tasks thanks to its tapered form and combined bending and suction features. This streamlined, high aspect ratio, multifunctional architecture thus enables the actuators to perform tasks in narrow and constrained conditions (Fig. 6D and Supplementary Movie S8), behaviors that are functionally similar to those observed in living octopus.[48]

While in this study, our actuators' designs mimic only the bending motion of an octopus arm, future prototypes could also incorporate three-dimensional (out of plane) bending and elongation,[54,55] material stiffness variability,[56–58] more structurally complex biomimetic suckers,[42,46] or the incorporation of reinforcing fibrous components[29,31] for added functionality. Additionally, the overall gripping performance of the actuators could be significantly enhanced by optimizing the sucker size and pattern for different arm taper angles. In the current study, because of the compact design of the actuators, we employed a simplified vacuum system to actuate the suckers, but we imagine that the *acetabular* contraction of the suckers could be more closely mimicked in future studies with different types of soft actuators, including those based on dielectric elastomers,[59,60] shape memory polymers,[61] or hydrogels.[40,62,63] It should also be noted that the arm's taper angle can be dynamically altered in living octopuses when catching prey items of different sizes or weights[64] and could, in theory, be replicated in our soft robotic analogs using some of the design strategies and materials systems outlined above. The results and diverse octopus-inspired design elements described here could thus help lay the foundation for the future design of dynamically morphable soft robots that can adapt in real time to perform specific tasks of interest.

Finally, our results also have implications for understanding the biomechanics of octopus arms. In nature, an octopus with a small arm taper angle (e.g., *O. macropus*, $3.58° \pm 0.33°$), and with a correspondingly thinner muscular structure, produces smaller bending radii to catch small preys compared with an octopus with a larger arm taper angle (e.g., *E. cirrhosa*, $9.32° \pm 1.66°$) with a thicker muscular structure.[65] The ecological and evolutionary consequences of this variability may be related to (1) size, strength, and speed of potential prey items, (2) habitat structural heterogeneity, or

(3) depth-dependent food availability and related octopus energetics. While the precise reasons for this observed diversity of arm taper angle are still largely unknown, the results reported here may shed new light on this matter and may stimulate further hypothesis testing into the various possibilities outlined above.

Acknowledgment

We would like to thank William Kier, Paul Valentich-Scott, and Eric Hochberg for helpful suggestions.

Author Disclosure Statement

L.W., Z.X., E.M.K., and Z.G. are inventors on the patent application (CN201710346369.1) submitted by Beihang University that covers the structure design of the tentacle gripper.

Funding Information

This work was supported by the National Science Foundation support projects, China (grant nos. 61822303, 61633004, 91848105 to L.W.) and the National Key Research and Development Program of China (no. 2018YFB1304604). K.B. gratefully acknowledges support by the National Science Foundation through grant DMREF-1533985 and the Wyss Institute for Biologically Inspired Engineering. Z.X. thanks the Innovation Foundation project YCSJ-03-2018-03 of Beihang University for PhD Graduates. Special thanks to Festo Corporate project for the financial support of the prototype development in the early stage.

Supplementary Material

Supplementary Data
Supplementary Movie S1
Supplementary Movie S2
Supplementary Movie S3
Supplementary Movie S4
Supplementary Movie S5
Supplementary Movie S6
Supplementary Movie S7
Supplementary Movie S8
Supplementary Movie S9

References

1. Laschi C, Mazzolai B, Cianchetti M. Soft robotics: technologies and systems pushing the boundaries of robot abilities. Sci Robot 2016;1:eaah3690.
2. Pfeifer R, Lungarella M, Iida F. Self-organization, embodiment, and biologically inspired robotics. Science 2007; 318:1088–1093.
3. Ijspeert AJ. Biorobotics: using robots to emulate and investigate agile locomotion. Science 2014;346:196–203.
4. Kizilkan E, Strueben J, Staubitz A, *et al.* Bioinspired photocontrollable microstructured transport device. Sci Robot 2017;2:eaak9454.
5. Koh JS, Yang E, Jung GP, *et al.* Jumping on water: surface tension-dominated jumping of water striders and robotic insects. Science 2015;349:517–521.
6. Wen L, Weaver JC, Lauder GV. Biomimetic shark skin: design, fabrication and hydrodynamic function. J Exp Biol 2014;217:1656–1666.
7. Wang Y, Yang X, Chen Y, *et al.* A biorobotic adhesive disc for underwater hitchhiking inspired by the remora suckerfish. Sci Robot 2017;2:eaan8072.
8. Domel AG, Saadat M, Weaver JC, *et al.* Shark skin-inspired designs that improve aerodynamic performance. J R Soc Interface 2018;15:20170828.
9. Vail AL, Manica A, Bshary R. Referential gestures in fish collaborative hunting. Nat Commun 2013;4:1765.
10. Richter JN, Hochner B, Kuba MJ. Octopus arm movements under constrained conditions: adaptation, modification and plasticity of motor primitives. J Exp Biol 2015;218:1069–1076.
11. Smith A. Cephalopod sucker design and the physical limits to negative pressure. J Exp Biol 1996;199:949–958.
12. Sumbre G, Gutfreund Y, Fiorito G, *et al.* Control of octopus arm extension by a peripheral motor program. Science 2001;293:1845–1848.
13. Margheri L, Laschi C, Mazzolai B. Soft robotic arm inspired by the octopus: I. From biological functions to artificial requirements. Bioinspir Biomim 2012;7:025004.
14. Laschi C, Mazzolai B. Lessons from animals and plants: the symbiosis of morphological computation and soft robotics. IEEE Robot Automat Mag 2016;23:107–114.
15. Calisti M, Giorelli M, Levy G, *et al.* An octopus-bioinspired solution to movement and manipulation for soft robots. Bioinspir Biomim 2011;6:036002.
16. Mazzolai B, Margheri L, Cianchetti M, *et al.* Soft-robotic arm inspired by the octopus: II. From artificial requirements to innovative technological solutions. Bioinspir Biomim 2012;7:025005.
17. Laschi C, Cianchetti M, Mazzolai B, *et al.* Soft robot arm inspired by the octopus. Adv Robot 2012;26:709–727.
18. Renda F, Cianchetti M, Giorelli M, *et al.* A 3D steady-state model of a tendon-driven continuum soft manipulator inspired by the octopus arm. Bioinspir Biomim 2012;7: 025006.
19. Giorelli M, Renda F, Calisti M, *et al.* Learning the inverse kinetics of an octopus-like manipulator in three-dimensional space. Bioinspir Biomim 2015;10:035006.
20. Grissom MD, Chitrakaran V, Dienno D, *et al.* Design and experimental testing of the octarm soft robot manipulator (Unmanned Systems Technology VIII, vol. 6230). Orlando, FL: International Society for Optics and Photonics, 2006, p. 62301F.
21. Walker ID, Dawson DM, Flash T, *et al.* Continuum robot arms inspired by cephalopods (Unmanned Ground Vehicle Technology VII, vol. 5804). Orlando, FL: International Society for Optics and Photonics, 2005, pp. 303–315.
22. Cianchetti M, Calisti M, Margheri L, *et al.* Bioinspired locomotion and grasping in water: the soft eight-arm OCTOPUS robot. Bioinspir Biomim 2015;10:035003.
23. Katzschmann RK, Marchese AD, Rus D. Autonomous object manipulation using a soft planar grasping manipulator. Soft Robot 2015;2:155–164.
24. Marchese AD, Rus D. Design, kinematics, and control of a soft spatial fluidic elastomer manipulator. Int J Robot Res 2016;35:840–869.
25. Rus D, Tolley MT. Design, fabrication and control of soft robots. Nature 2015;521:467.
26. Majidi C. Soft robotics: a perspective—current trends and prospects for the future. Soft Robot 2014;1:5–11.
27. Shepherd RF, Stokes AA, Nunes RMD, *et al.* Soft machines that are resistant to puncture and that self seal. Adv Mater 2013;25:6709–6713.

28. Mosadegh B, Polygerinos P, Keplinger C, *et al.* Pneumatic networks for soft robotics that actuate rapidly. Adv Funct Mater 2014;24:2163–2170.
29. Polygerinos P, Wang Z, Overvelde JTB, *et al.* Modeling of soft fiber-reinforced bending actuators. IEEE Trans Robot 2015;31:778–789.
30. Ranzani T, Gerboni G, Cianchetti M, *et al.* A bioinspired soft manipulator for minimally invasive surgery. Bioinspir Biomim 2015;10:035008.
31. Connolly F, Walsh CJ, Bertoldi K. Automatic design of fiber-reinforced soft actuators for trajectory matching. Proc Natl Acad Sci 2017;114:51–56.
32. Kwok SW, Morin SA, Mosadegh B, *et al.* Magnetic assembly of soft robots with hard components. Adv Funct Mater 2014;24:2180–2187.
33. Deimel R, Brock O. A novel type of compliant and underactuated robotic hand for dexterous grasping. Int J Robot Res 2016;35:161–185.
34. Shepherd RF, Ilievski F, Choi W, *et al.* Multigait soft robot. Proc Natl Acad Sci 2011;108:20400–20403.
35. Terryn S, Brancart J, Lefeber D, *et al.* Self-healing soft pneumatic robots. Sci Robot 2017;2:eaan4268.
36. Brojan M, Videnic T, Kosel F. Large deflections of nonlinearly elastic non-prismatic cantilever beams made from materials obeying the generalized Ludwick constitutive law[J]. Meccanica 2009;44:733–739.
37. Baik S, Park Y, Lee T J, *et al.* A wet-tolerant adhesive patch inspired by protuberances in suction cups of octopi. Nature 2017;546:396.
38. Hou J, Wright E, Bonser RHC, *et al.* Development of biomimetic squid-inspired suckers. J Bionic Eng 2012;9:484–493.
39. Choi MK, Park OK, Choi C, *et al.* Cephalopod-inspired miniaturized suction cups for smart medical skin. Adv Health Mater 2016;5:80–87.
40. Lee H, Um DS, Lee Y, *et al.* Octopus-inspired smart adhesive pads for transfer printing of semiconducting nanomembranes. Adv Mater 2016;28:7457–7465.
41. Lucas KN, Johnson N, Beaulieu WT, *et al.* Bending rules for animal propulsion. Nat Comm 2014;5:3293.
42. Tramacere F, Beccai L, Kuba MJ, *et al.* Octopus suckers identification code (OSIC). Mar Freshw Behav Physiol 2013;46:447–453.
43. Kier WM, Smith AM. The morphology and mechanics of octopus suckers. Biol Bullet 1990;178:126–136.
44. Kier WM, Smith AM. The structure and adhesive mechanism of octopus suckers. Integr Comp Biol 2002;42:1146–1153.
45. Gent AN. A new constitutive relation for rubber. Rub Chem Tech 1996;69:59–61.
46. Tramacere F, Follador M, Pugno NM, *et al.* Octopus-like suction cups: from natural to artificial solutions. Bioinspir Biomim 2015;10:035004.
47. Han JY. Low-cost multi-touch sensing through frustrated total internal reflection. In: Proceedings of the 18th Annual ACM Symposium on User Interface Software and Technology. ACM, 2005, pp. 115–118.
48. Caldwell RL, Ross R, Rodaniche A, *et al.* Behavior and body patterns of the larger Pacific striped octopus. PloS One 2015; 10:e0134152.
49. Autumn K, Liang YA, Hsieh ST, *et al.* Adhesive force of a single gecko foot-hair. Nature 2000;405:681.
50. Song S, Drotlef DM, Majidi C, *et al.* Controllable load sharing for soft adhesive interfaces on three-dimensional surfaces. Proc Natl Acad Sci 2017;114:E4344–E4353.
51. Glick P, Suresh SA, Ruffatto D, *et al.* A soft robotic gripper with gecko-inspired adhesive. IEEE Robot Autom Lett 2018;3:903–910.
52. Li J, Celiz AD, Yang J, *et al.* Tough adhesives for diverse wet surfaces. Science 2017;357:378–381.
53. Hao Y, Gong Z, Xie Z, *et al.* Universal soft pneumatic robotic gripper with variable effective length. In: 2016 35th Chinese Control Conference (CCC). IEEE 2016, pp. 6109–6114.
54. Robertson MA, Paik J. New soft robots really suck: vacuum-powered systems empower diverse capabilities. Sci Robot 2017;2:eaan6357.
55. Kim SJ, Lee DY, Jung GP, *et al.* An origami-inspired, self-locking robotic arm that can be folded flat. Sci Robot 2018; 3:eaar2915.
56. Bartlett NW, Tolley MT, Overvelde JTB, *et al.* A 3D-printed, functionally graded soft robot powered by combustion. Science 2015;349:161–165.
57. Elsayed Y, Vincensi A, Lekakou C, *et al.* Finite element analysis and design optimization of a pneumatically actuating silicone module for robotic surgery applications. Soft Robot 2014;1:255–262.
58. Lekakou C, Elsayed Y, Geng T, *et al.* Skins and sleeves for soft robotics: inspiration from nature and architecture. Adv Eng Mater 2015;17:1180–1188.
59. Shian S, Bertoldi K, Clarke DR. Dielectric elastomer based ''grippers'' for soft robotics. Adv Mater 2015;27:6814–6819.
60. Shintake J, Rosset S, Schubert B, *et al.* Versatile soft grippers with intrinsic electroadhesion based on multifunctional polymer actuators. Adv Mater 2016;28:231–238.
61. Zhao Z, Zhang K, Liu Y, *et al.* Highly stretchable, shape memory organohydrogels using phase-transition microinclusions. Adv Mater 2017;29:1701695.
62. Fu F, Shang L, Chen Z, *et al.* Bioinspired living structural color hydrogels. Sci Robot 2018;3:eaar8580.
63. Kim YS, Liu M, Ishida Y, *et al.* Thermoresponsive actuation enabled by permittivity switching in an electrostatically anisotropic hydrogel. Nat Mater 2015;14:1002.
64. Kier WM, Stella MP. The arrangement and function of octopus arm musculature and connective tissue. J Morphol 2007;268:831–843.
65. Steer MA, Semmens JM. Pulling or drilling, does size or species matter? An experimental study of prey handling in *Octopus dierythraeus*. J Exp Marine Biol Ecol 2003;290:165–178.

Address correspondence to:
Li Wen
School of Mechanical Engineering and Automation
Beihang University
Beijing 100083
China

E-mail: liwen@buaa.edu.cn

Katia Bertoldi
John A. Paulson School of Engineering
and Applied Sciences
Harvard University
Cambridge, MA 02138

E-mail: bertoldi@seas.harvard.edu